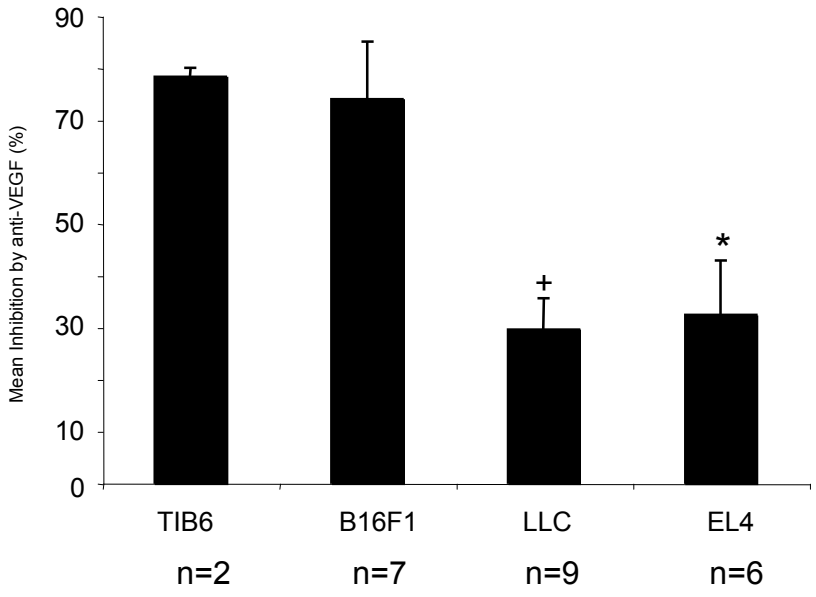

Supplemental Figure 1 Differential growth inhibition by anti-VEGF treatment. The percent of tumor growth inhibition was calculated on the basis of tumor volumes in anti-VEGF vs. control treated mice in each tumor type at day 14. We chose day 14 for analysis since in some experiments, some of the tumor bearing mice had to be euthanized. “n” indicates the number of independent experiments performed. In each experiment, five mice were treated with anti-VEGF or control antibodies. Bars represent mean of tumor growth inhibition (%) ± SEM. * Indicates that the difference between EL4 and B16F1 or TIB6 tumors is significant ($p<0.05$). + Indicates a significant difference between LLC ($p<0.05$) and B16F1 or TIB6 tumors.

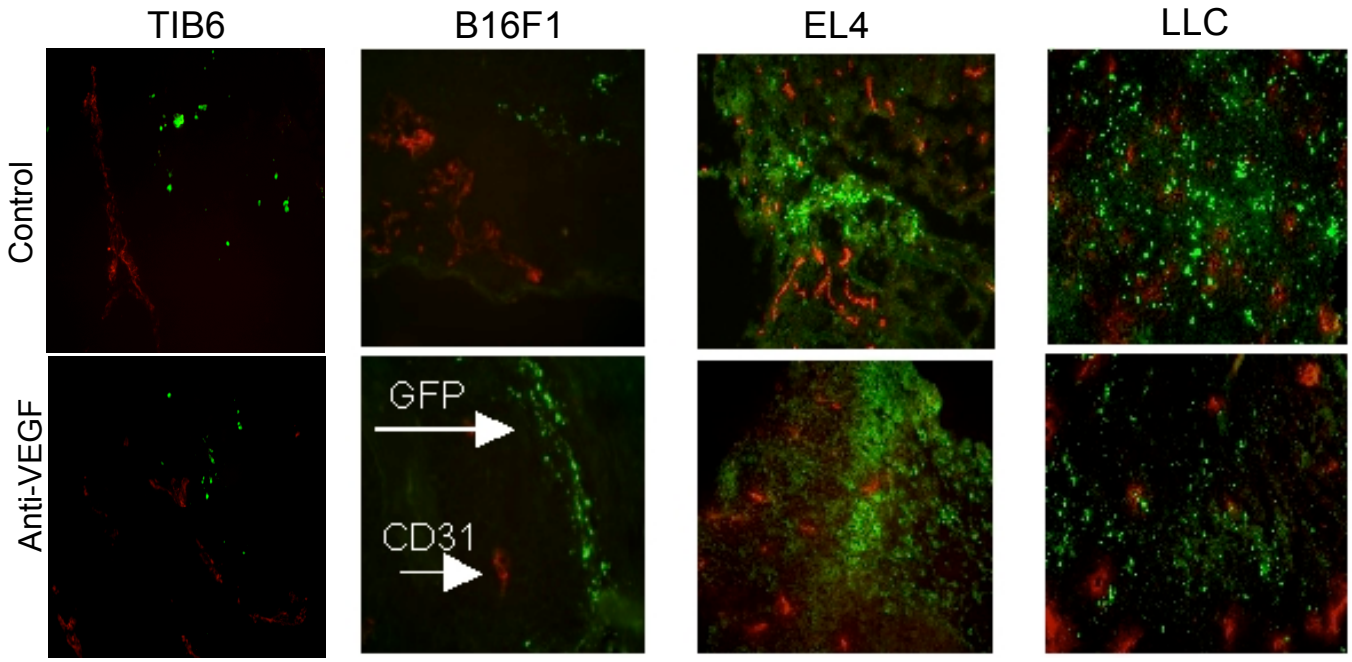

Supplemental Figure 2 Infiltration of GFP+ cells in refractory tumors. Immunofluorescent staining of CD31+ (red) and GFP+ cells (green) in TIB6, B16F1, EL4 and LLC tumor sections isolated from mice treated with control or anti-VEGF antibodies as described in Fig.1a. The vast majority of GFP+ cells are devoid of CD31 expression, indicating that BMMNCs do not directly contribute to the tumor vasculature in our models.

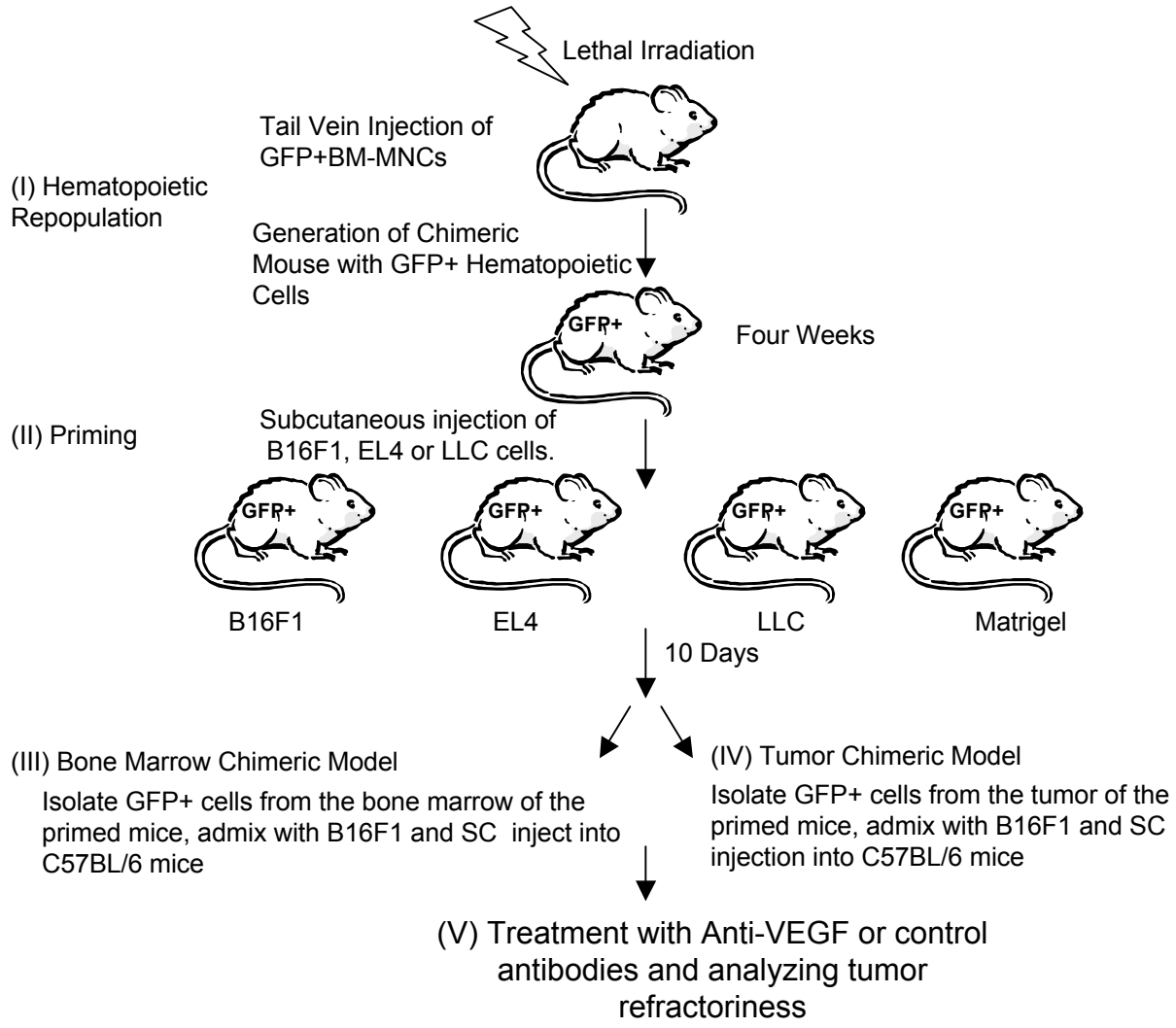

Supplemental Figure 3 Strategies to investigate the role of BMMNCs in tumor refractoriness to anti-VEGF treatment. To monitor kinetics of BMMNCs in tumor bearing animals, GFP+BMMNCs were intravenously injected into lethally irradiated C57BL/6 mice (I). Next, the chimeric mice were primed by implantation of sensitive (B16F1) and refractory (EL4 and LLC) tumors in matrigel (II). GFP+ cells from both BM (III) or tumors (IV) of chimeric mice were isolated, admixed with B16F1 cells and were then injected sc into C57BL/6 mice. Implanted animals were treated with anti-VEGF or control antibodies and the role of BMMNCs in mediating tumor refractoriness to anti-VEGF treatment was investigated (V).

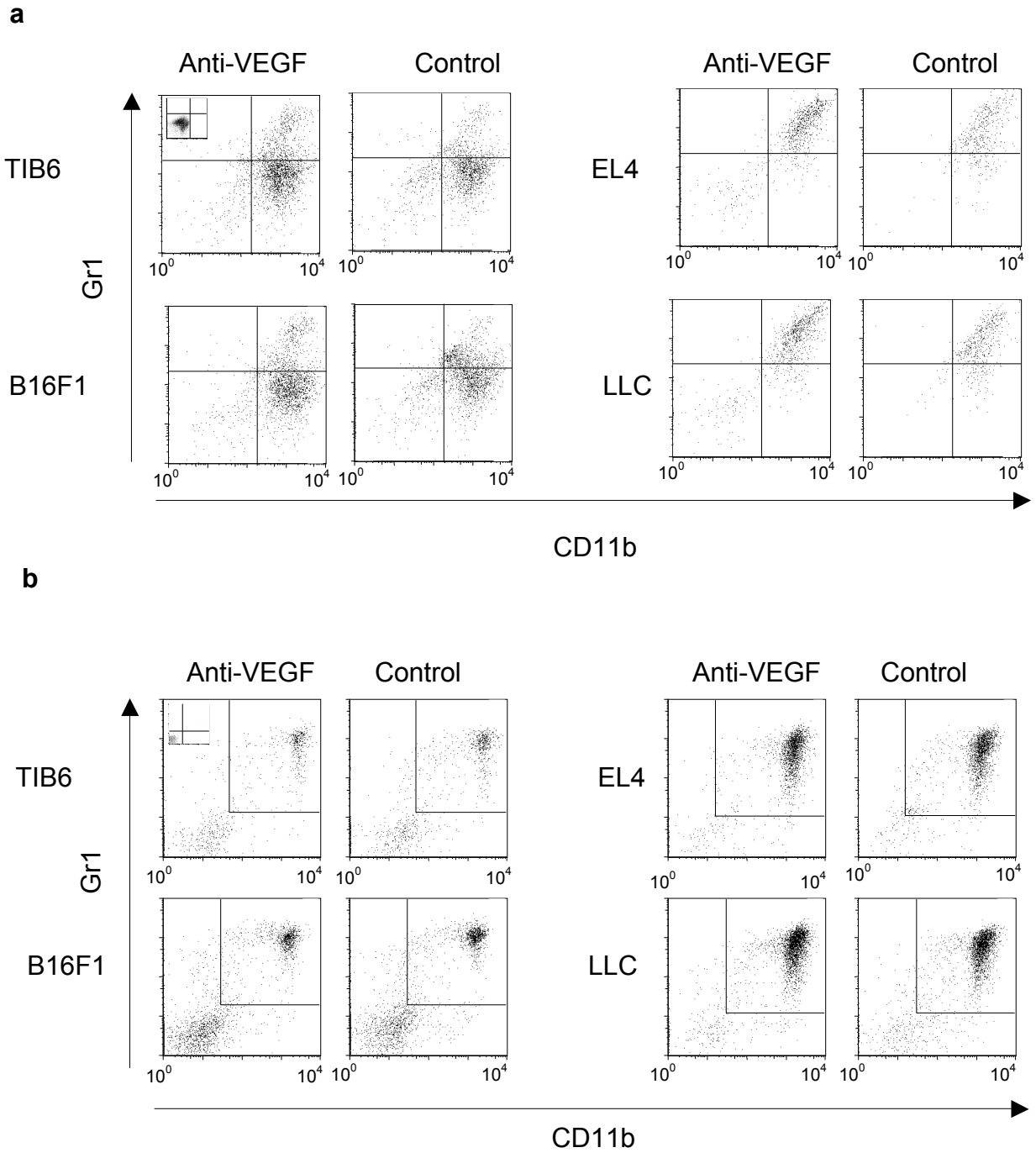

Supplemental Figure 4 FACS profile representative of CD11b+Gr1+ cells in the tumors and BM of mice bearing refractory or sensitive tumors. The myeloid compartments in mice bearing TIB6, B16F1, EL4 and LLC tumors were analyzed using a FACS machine and monoclonal antibodies against CD11b and Gr1. Displays are the representative CD11b+Gr1+ subset in the tumors **(a)** and the BMs **(b)**.

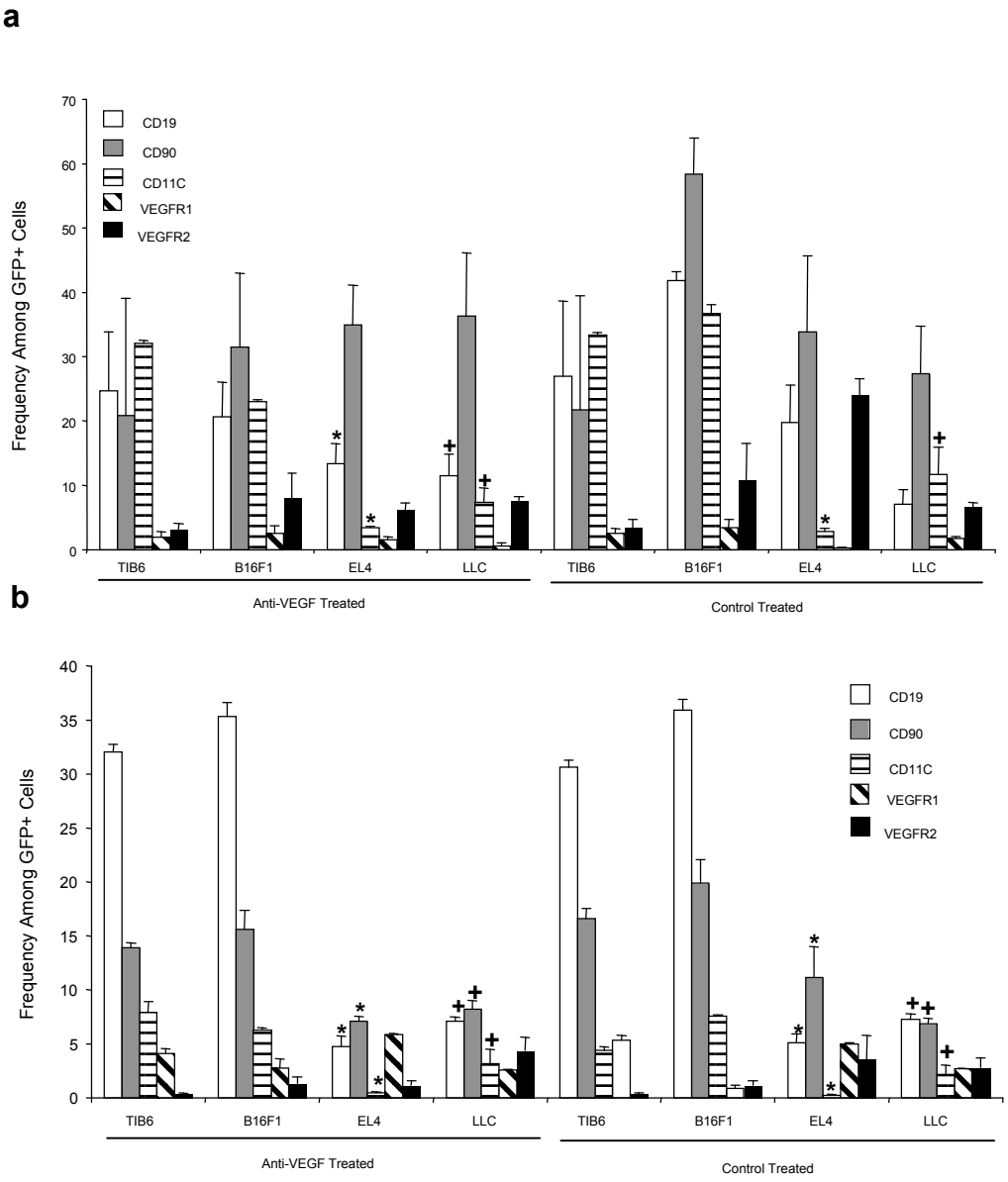

Supplemental Figure 5 Multilineage analysis of GFP+ cells in the tumor and BM in mice bearing refractory or sensitive tumors. C57BL/6 mice were implanted with TIB6, B16F1, EL4 and LLC tumors and were treated with anti-VEGF or control antibodies as described. BMMNCs and tumor isolates were harvested from each mouse and were stained with antibodies against CD19 (B lymphoid), CD90 (T lymphoid), CD11c (dendritic) and also VEGF receptors (R1 and R2). Graphs represent the frequency of each subset in the tumors **(a)** and in the BM **(b)** compartments. *indicates that the difference between EL4 and B16F1 or TIB6 tumor bearing animals is significant ($p<0.05$). **+** Indicates a significant difference ($p<0.05$) between LLC and B16F1 or TIB6 tumor bearing animals.

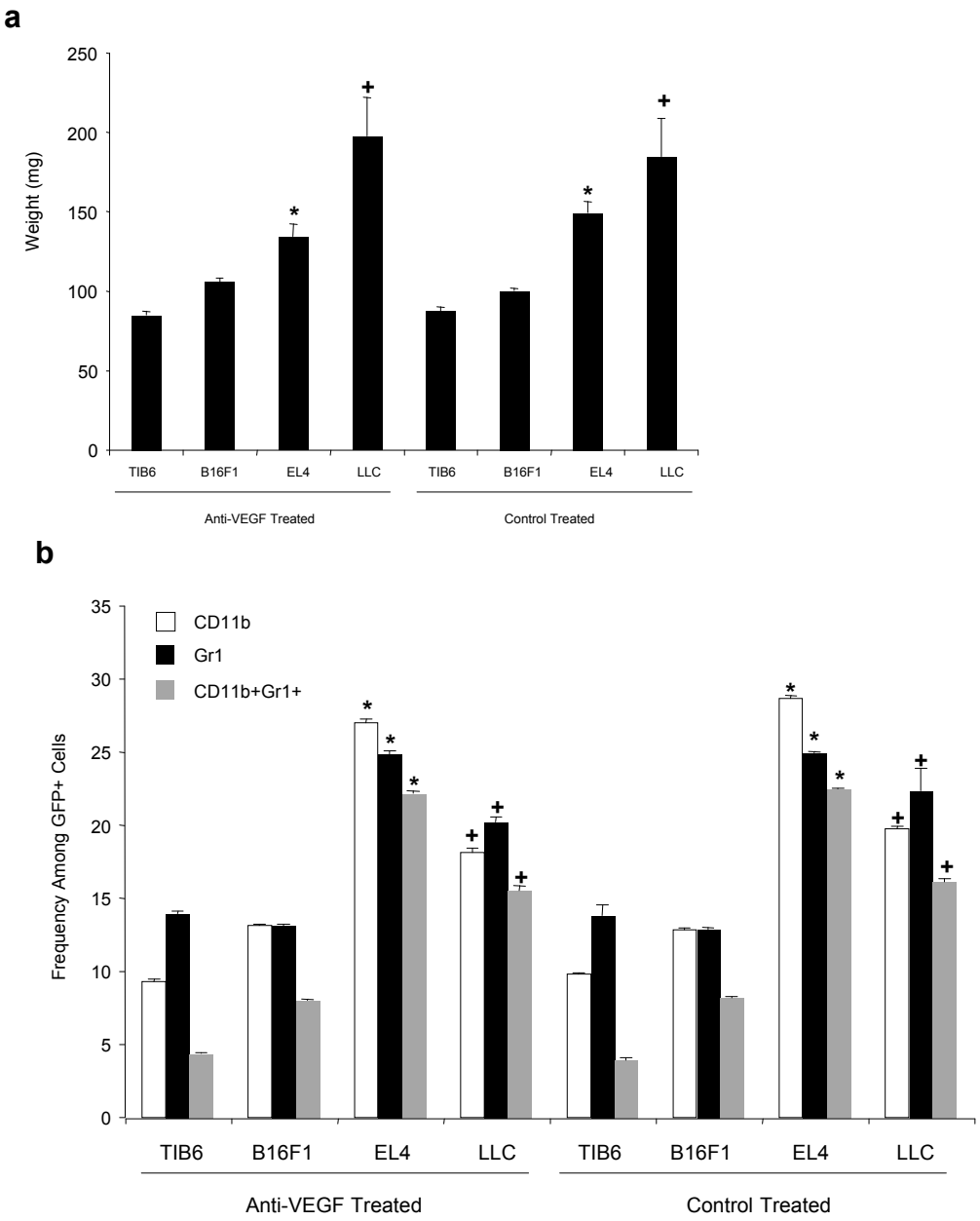

Supplemental Figure 6 The spleen is an alternative site of homing for CD11b+Gr1+cells in mice bearing refractory tumors. C57BL/6-GFP chimeric mice were implanted with TIB6, B16F1, EL4 or LLC tumors and were treated with anti-VEGF or control antibodies for 17 days, as described. **(a)** The spleen of mice bearing refractory tumors was significantly ($p<0.05$) larger than the spleen of mice bearing sensitive tumors **(b)** Splenocytes were harvested from each mouse using mechanical disruption and were treated with lysis buffer to remove red blood cells. Spleen cells were then stained with anti-CD11b and anti-Gr1 antibodies and were then analyzed by FACS to investigate the frequency of CD11b+Gr1+ cells. A significant increase ($p<0.05$) in the frequency of CD11b+Gr1+ cells in the spleen of mice bearing refractory tumor compared to the sensitive tumors was found. * Indicates that the difference between EL4 and B16F1 or TIB6 tumors is significant ($p<0.05$). **+** Indicates a significant difference ($p<0.05$) between LLC and B16F1 or TIB6 tumors.

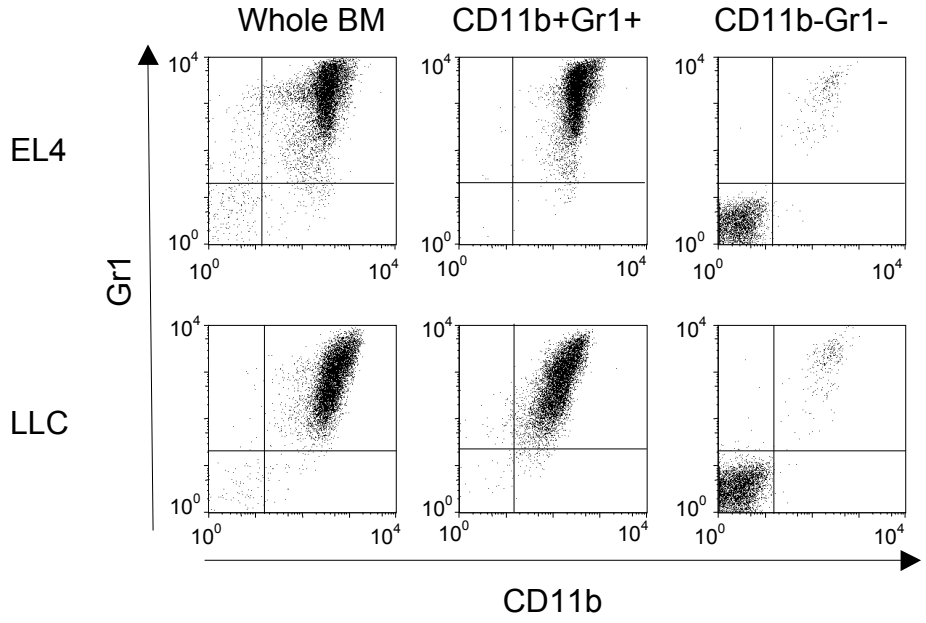

Supplemental Figure 7 Purification of CD11b+Gr1+ from the BM C57BL/6 mice of mice implanted with EL4 or LLC tumors. BMMNCs were labeled with CD11b conjugated beads and passed through large-scale magnetic columns to isolate CD11b+ and CD11b- fractions. An aliquot from each fraction as well as unsorted cells were stained with CD11b and Gr1 fluorochrome conjugated antibodies to ensure the purity of the population of interest in each subset.

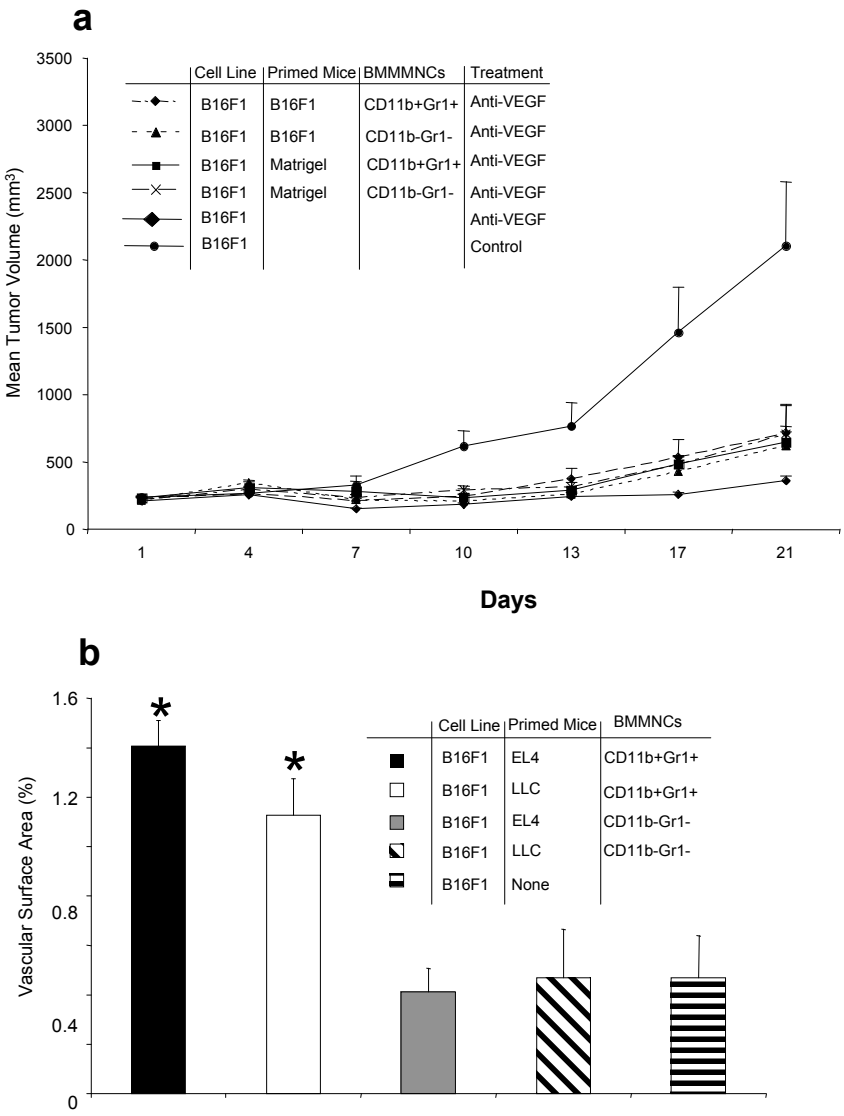

Supplemental Figure 8 (a) Myeloid cells isolated from mice primed with sensitive tumors fail to induce refractoriness to anti-VEGF. The graph shows growth curves of B16F1 tumors admixed with B16F1- or matrigel-primed, BM-CD11b+Gr1+cells and treated with anti-VEGF (*n*=5 per group). The experiments were performed at the same time as those shown in Fig. 3d. Therefore, the control is common to both figures. Tumor volumes were measured for up to 21 days after implantation, as described. **(b)** Induction of angiogenesis by CD11b+Gr1+ cells is one the mechanisms leading to refractoriness to anti-VEGF treatment. VSAs were analyzed in mice harboring admixture of B16F1 and CD11b+Gr1+or CD11b-Gr1- cells. * Indicates significant difference ($p<0.05$) when comparing admixture of B16F1 and CD11b+Gr1+ cells from EL4 or LLC primed mice to B16F1 admixture with CD11b-Gr1- cells isolated from the same primed animals.

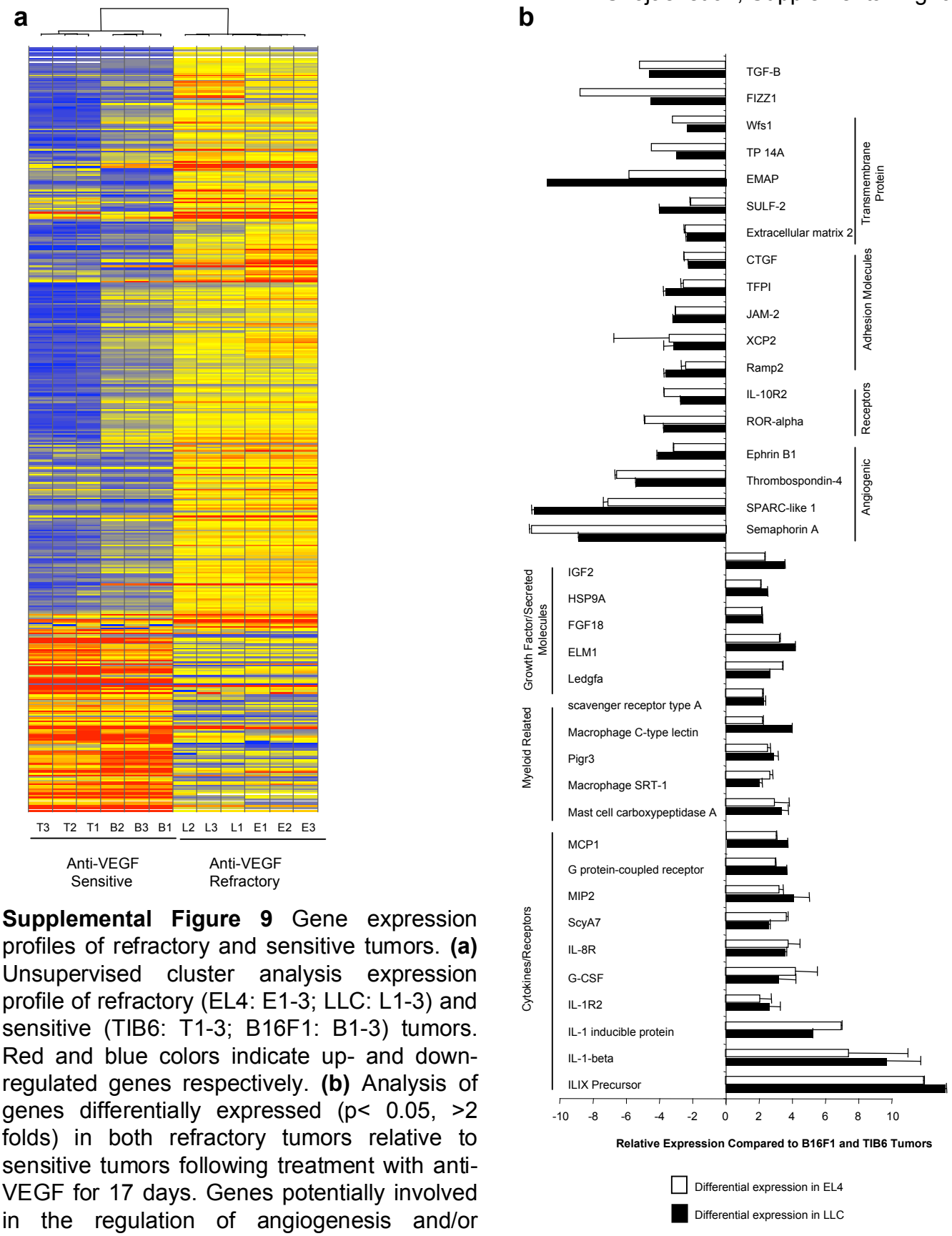

Supplemental Figure 9 Gene expression profiles of refractory and sensitive tumors. **(a)** Unsupervised cluster analysis expression profile of refractory (EL4: E1-3; LLC: L1-3) and sensitive (TIB6: T1-3; B16F1: B1-3) tumors. Red and blue colors indicate up- and down-regulated genes respectively. **(b)** Analysis of genes differentially expressed ($p < 0.05$, >2 folds) in both refractory tumors relative to sensitive tumors following treatment with anti-VEGF for 17 days. Genes potentially involved in the regulation of angiogenesis and/or hematopoietic properties of myeloid cells such as growth factors, cytokines and adhesion molecules are displayed.

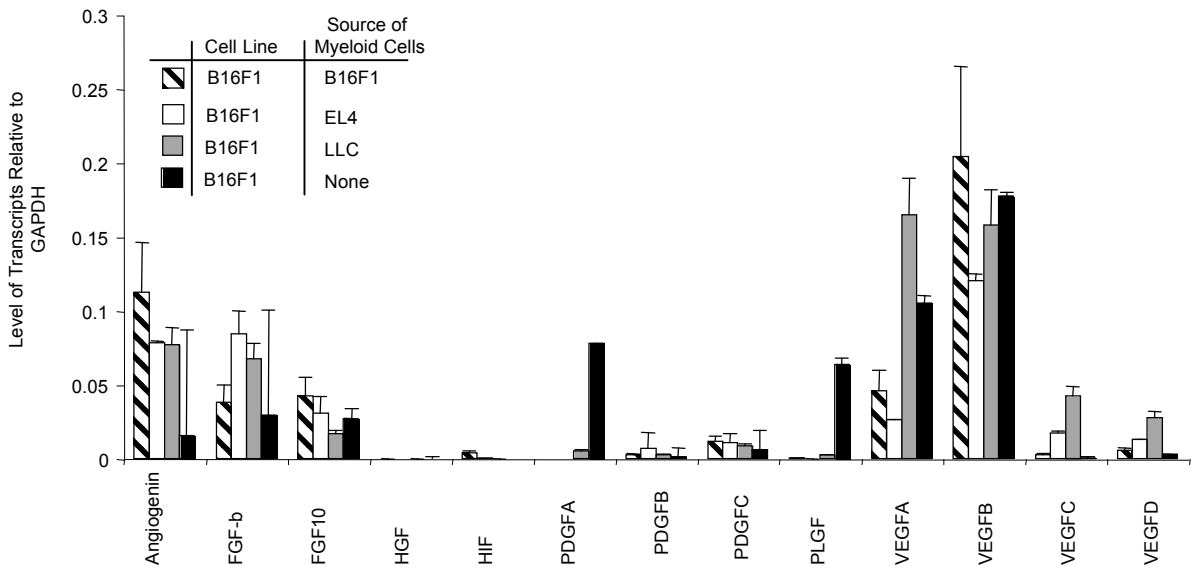

Supplemental Figure 10 Expression of angiogenic factors in sensitive tumors admixed with myeloid cells isolated from refractory- or sensitive-tumor primed mice. Admixtures of B16F1 tumor cells and myeloid cells were harvested from C57BL/6 mice which had been treated with anti-VEGF. Total RNA was extracted as described, and the expression levels of some of the known angiogenic transcripts including *Angiogenin, bFGF, FGF10, HGF, HIF, PDGFA, PDGFB, PDGFC, PLGF, VEGFA, VEGFB, VEGFC and VEGFD* were evaluated using Taqman PCR.

Supplemental Table 1. Sequences of primers in Taqman PCR

Transcript	Forward Primer	Reverse Primer	Taqman Primer
VEGFA	TGTACCTCCACCCTGCCAAGT	TGGAAGATGTCCACCAGGGT	CCAGCGAAGCTACTGCCGTCCAATT
VEGFB	GACGATGGCCTGGAATGT	GGTACTTGGATCATGAGGATCTG	CACTGGGCAACACCAAGTCCG
VEGFC	CCACTAAAAATATTGTTCCTGCAT	TGATCACAGTGAGCTTTACCAAT	CCACTAAAAATATTGTTCCTGCATTCATTTTTATAGCA
VEGFD	TTGACCTAGTGTCATGGTAAAGC	TCAGTGAACTGGGGAATCAC	ACATTTCCATGCAATGGCGGCT
PDGFA	CGTGTGACATTCCTGAACATACTA	GTCCTCGGACACGGTTTT	CAATGTGCGTGCGGTCTTTGTTCT
PDGFB	CAATGCCGGGCCTCG	TCGCACAATCTCAATCTTTCTCA	CTCGATGCCTGATTCGGACGGC
PDGFC	TTTGCTTGTAAAATGCTTAATATCG	CCCAAAATAGCCACATTCTTTTA	TTGATTCAAATAGTCACCACATAA CCTAGGCA
Angiogenin	ACCACCATTAGCGCCATGTT	CATATTTACGTGCCATGAAGAA	TAGGGTGGTGCACTCAGCGCCG
HIF-1α	GCCCCAGATTCAGGATCAGA	TGGGACTATTAGGCTCAGGTGAAC	CCTAGTCCTTCCGATGGAAGCACTAG ACAA
HGF	GGCCCACTCATTTGTGAAC	CATCCACGACCAGGAAC	ACACAAAATGAGAATGGTTCTTGGTGTCA
PLGF	GCAGTAGCCCGTGGACTT	CGGTCCAGGTCTTCCACCAACTG	ACACACACCCAGACTTGTATCGGTCA
FGF-b	CCTCTCAGAGACCTACGTTCAA	GGAGGTCAAGGCCACAAT	CGGTCCAGGTCTTCCACCAACTG
FGF10	CTTGCCACAGGTCACAATG	GCCTTACAAAGGGCTCATGT	TGTGCAGATAACCTTTGCATCATTTGC
GAPDH	ATGTTCCAGTATGACTCCACTTCACG	GAAGACACCAGTAGACTCCACGACA	AAGCCCATCACCATCTTCCAGGAGCGAGA